Theor Chem Acc (2006) 115: 100–112
DOI 10.1007/s00214-005-0056-2

REGULAR ARTICLE

**Charles W. Bock · George D. Markham · Amy K. Katz**
**Jenny P. Glusker**

# The arrangement of first- and second-shell water molecules around metal ions: effects of charge and size

Received: 5 June 2005 / Accepted: 4 August 2005 / Published online: 11 February 2006


**Abstract** Structural features of clusters involving a metal ion ($Li^+$, $Na^+$, $Be^{2+}$, $Mg^{2+}$, $Zn^{2+}$, $Al^{3+}$, or $Ti^{4+}$) surrounded by a total of 18 water molecules arranged in two or more shells have been studied using density functional theory. Effects of the size and charge of each metal ion on the organization of the surrounding water molecules are compared to those found for a $Mg\,[H_2O]_6^{2+} \bullet [H_2O]_{12}$ cluster that has the lowest known energy on the $Mg^{2+} \bullet [H_2O]_{18}$ potential energy surface (Markham et al. in J Phys Chem B 106:5118–5134, 2002). The corresponding clusters with $Zn^{2+}$ or $Al^{3+}$ have similar structures. In contrast to this, clusters with a monovalent $Li^+$ or $Na^+$ ion, or with a very small $Be^{2+}$ ion, differ in their hydrogen-bonding patterns and the coordination number can decrease to four. The tetravalent $Ti^{4+}$ ionizes one inner-shell water molecule to a hydroxyl group leaving a $Ti^{4+}\,(H_2O)_5\,(OH^-)$ core, and an $H_3O^+ \bullet \bullet \bullet H_2O$ moiety dissociates from the second shell of water molecules. These observations highlight the influence of cation size and charge on the local structure of hydrated ions, the high-charge cations causing chemical changes and the low-charge cations being less efficient in maintaining the local order of water molecules.

**Keywords** Metal ion · Cation hydration · Density functional theory · Second hydration shell · Water structure · Hydrogen bonding network

**Electronic Supplementary Material:** Supplementary material is available for this article at http://dx.doi.org/10.1007/S00214-005-0056-2.

C.W. Bock
Philadelphia University, Henry Avenue and Schoolhouse Lane, Philadelphia, PA 19144-5497, USA

C.W. Bock · G.D. Markham · A.K. Katz · J.P. Glusker (✉)
The Institute for Cancer Research, Fox Chase Cancer Center, 333 Cottman Avenue, Philadelphia, PA 19111-2497, USA
E-mail: JP_Glusker@fccc.edu

A.K. Katz
The University of Tennessee School of Genome Science and Technology, F337 Walters Life Sciences Building, 1414 West Cumberland Avenue, Knoxville, TN 37996-0845, USA

## 1 Introduction

Many physico- and biochemical processes are directly controlled, or indirectly conditioned, by metal ions. These effects often require the desolvation of the metal ion, which is considered to exist as a metal–solvent cluster in solution. Metal ions are hydrated to varying degrees in aqueous solution [1–3]. This hydration typically is described as occurring in shells, with the nature of the inner shell (first coordination sphere) being determined to a large extent by the chemical and physical properties of the central metal ion (e.g., size, charge, electronic state, etc.). Additional shells of water result from hydrogen bonding with the inner-shell water molecules, as well as from long-range electrostatic effects from the metal ion. These additional shells begin the interface between the immediate metal ion environment and that of bulk water. Presumably the energetic penalty for rearranging the local water structure to afford ion solvation is minimized by limiting the disruption of the three-dimensional structure of bulk water.

In this article we describe investigations of the possible structures of hydration shells around several metal ions, and the effects that the size and charge of the central cation have on the structure of these shells. Aqueous solutions of metal ions certainly involve a myriad of fluctuating arrangements of the surrounding water molecules, but the structures of the predominant species, particularly with respect to the second hydration shell, are not known for most metal ions [4]. Molecular dynamics (MD) simulations provide an important theoretical tool with which to study the dynamics of water molecules in the shells surrounding a metal cation [5,6]. In particular, quantum mechanics/molecular mechanics (QM/MM) MD methods, which reliably correct for the effects of many-body interactions, are providing important insights into the variety of species present in metal ion–water systems and their kinetic stability [7,8].

In a complementary approach, we have employed cluster calculations using density functional theory (DFT) to investigate static patterns involved in the water arrangements surrounding metal ions when several hydration shells are

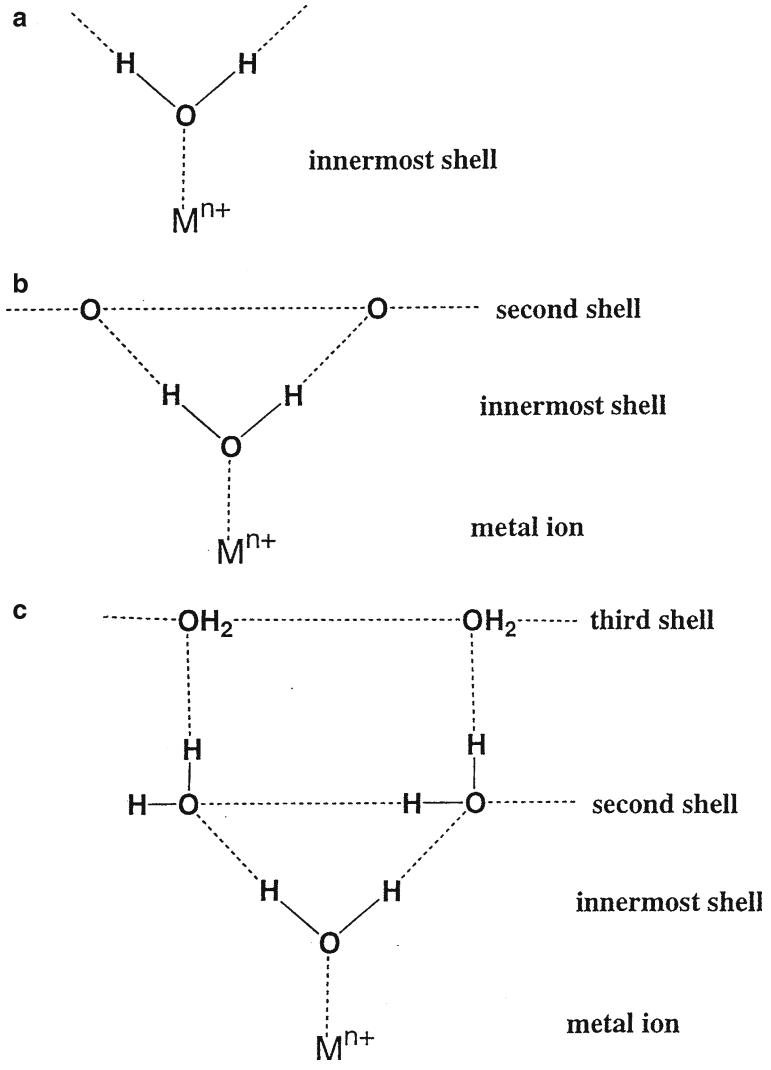


**Fig. 1** Hydrogen-bonding patterns in metal ion–water clusters

present [9,10]. Computational studies of metal ion–water complexes, with explicit inclusion of a second complete (or nearly complete) coordination shell, have been impractical until recently and are still relatively rare [9–14]. In 2002 we reported an extensive computational study of the structures and energies of several $Mg^{2+}\,[H_2O]_{18}$ clusters [9]. Divalent magnesium was chosen as our "reference" ion because it is biologically important, existing predominantly in one charge state, and there is a good agreement from a variety of experimental and computational studies that its inner hydration sphere includes six water molecules [9,15–21]. Furthermore, the mean residence time (MRT) of a water molecule in the inner shell, approximately $10^{-6}$s, is relatively long, substantiating the presence of metastable structures [1,7,22]. The $Mg\,[H_2O]_6^{2+}$ octahedral structural motif is also found in the crystal structures of magnesium complexes in which the Mg • • • O distances are 2.0–2.1 Å and Mg • • • O–H angles are near 127° [23–25]. The six water molecules of the inner shell are oriented with their oxygen atoms pointing toward the metal ion and the more positively charged hydrogen atoms are directed away from the charged cation, as shown in Fig. 1a [26]. These hydrogen atoms can then form hydrogen bonds to oxygen atoms of second-shell water molecules (see Fig. 1b, c). Much less is known experimentally about the second hydration shell around $Mg^{2+}$, either in solution or in crystal structures, but at least 12 water molecules are likely to be hydrogen bonded to the 6 water molecules in the inner shell.

Since the global minimum on the potential energy surface (PES) of an isolated $Mg\,[H_2O]_6^{2+}$ cluster has $T_h$ symmetry [9, 25], one might have anticipated that the global minimum on the $Mg\,[H_2O]_6^{2+} \bullet [H_2O]_{12}$ PES would also have $T_h$ symmetry [27]. However, calculations have shown that this $T_h$ structure is not even a local minimum on the PES, and thus the global minimum has a different symmetry [9,14].

Pye and Rudolph [14] were the first to locate a true local minimum on the $Mg\,[H_2O]_6^{2+} \bullet [H_2O]_{12}$ PES in their

computational studies at the HF/6-31G*//HF/6-31G* level. The structure of their cluster is quite novel. It has $T$ symmetry and the Mg $[H_2O]_6^{2+}$ moiety effectively interacts with four distinct (cyclic) water trimers in the second shell; more recently, we have confirmed that this structure is also stable at the B3LYP/6-31+G**//B3LYP/6-31+G** level [9]. Subsequently, however, we located a different structure of the Mg $[H_2O]_6^{2+} \bullet [H_2O]_{12}$ cluster, see Fig. 2, that is 8.3 kcal/mol lower in energy than the $T$ symmetry form at the same B3LYP level; it has approximately $S_6$ symmetry and, to date, it is the lowest-energy local minimum that has been found on the Mg $[H_2O]_6^{2+} \bullet [H_2O]_{12}$ PES [9]. The structure of this complex is not spherical, but is flattened at the two poles, see Fig. 3 in [9]. The integrated hydrogen-bonded network found in this cluster consists of pentameric subunits comprised of four water molecules from the second shell and one from the first shell; the average Mg•••O distance to a water molecule in the second shell is 4.13 Å, compared to 2.10 Å for the first shell at the B3LYP/6-31+G** level [9]. In an earlier study Uudsemaa and Tamm [11] had found a similar type of $S_6$ cluster in their computational studies of $Ti^{3+}$ complexes surrounded by 18 water molecules; for this study they employed the Becke–Perdew BP86 functional with a split-valence basis set and polarization functions on the non-hydrogen atoms [28,29]. The "flat" structure of these $S_6$ clusters suggests that one or two additional water molecules could loosely bind to them and consequently be classified as part of the second shell based on distance criteria. Indeed, the 200 ps MD simulation of Martinez et al. [30], which involved one $Mg^{2+}$ ion, six first-shell water molecules and 512 TIP4P water molecules that act as the solvent [31], found a second-shell coordination number (CN) of 13; the average Mg•••O distance to a water molecule in the second shell during the simulation was estimated to be 4.25 Å .

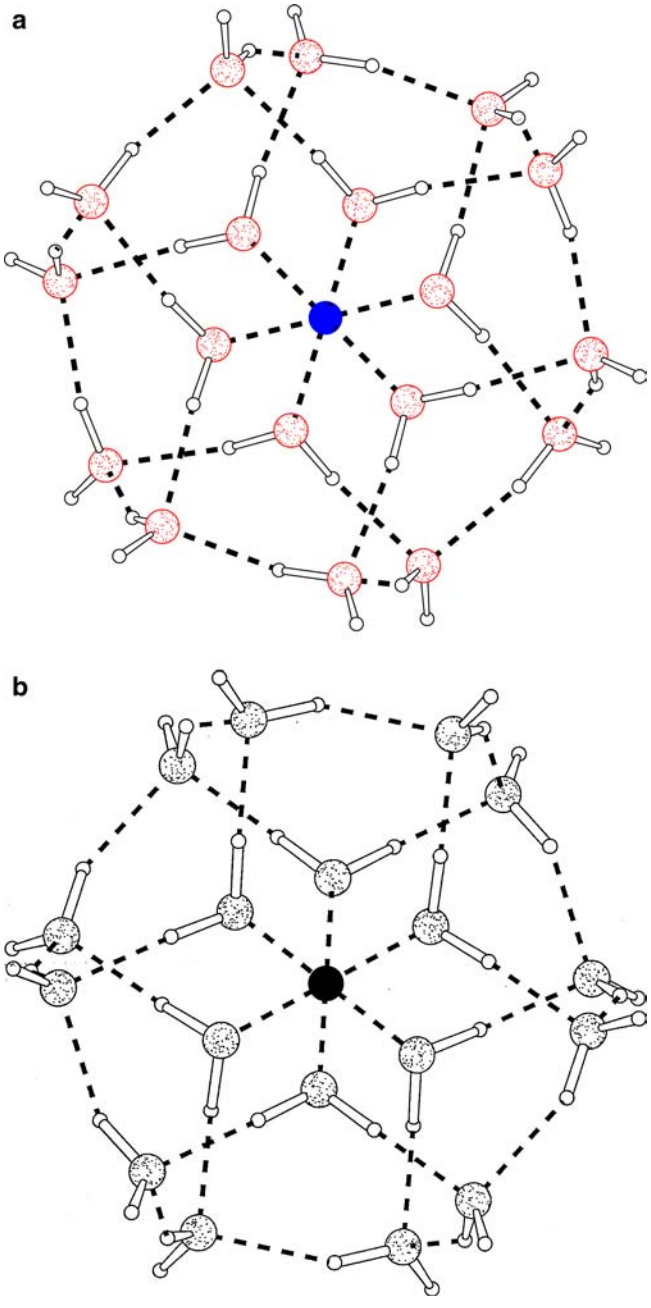


**Fig. 2** Optimized structures of **(a)** the Mg $[H_2O]_6^{2+} \bullet [H_2O]_{12}$ ($S_6$) reference cluster obtained at the B3LYP/6-31+G** computational level [9], and **(b)** the Al $[H_2O]_6^{3+} \bullet [H_2O]_{12}$ obtained at the B3LYP/6-31+G** computational level

In this article we report the effects of cation replacement on a hydrogen-bonded network of the cluster of a single metal ion and 18 water molecules. We analyzed the effects of replacing the central divalent magnesium ion (ionic radius = 0.65 Å) in the B3LYP/6-31+G**-optimized Mg $[H_2O]_6^{2+} \bullet [H_2O]_{12}$ ($S_6$) cluster by either a $Li^+$ (0.60 Å), $Na^+$ (0.95 Å), $Be^{2+}$ (0.31 Å), $Zn^{2+}$ (0.74 Å), $Al^{3+}$ (0.50 Å), or $Ti^{4+}$ (0.68 Å) ion [32]. In each case the resulting cluster was reoptimized at the same computational level. The variety of charges, ionic radii, and electronic structures of the metal ions included in this study provide a broad perspective on competing influences that affect the arrangement of surrounding water molecules.

We also compare our computational results with experimental data from crystal structures that contain hydrated metal ions; these data were taken from the Cambridge Structural Database (CSD) [33]. Our results provide information on preferred CNs for the metal ions in this study, as well as data on the organization of water shells around metal ions in the solid state as found from X-ray and neutron diffraction studies.

## 2 Computational methodology

Equilibrium geometries and vibrational frequencies of the 18-water clusters discussed in this article were predicted using the B3LYP method; B3LYP employs a three-parameter HF/DFT hybrid exchange functional (B3) [34], coupled with the dynamical correlation functional of Lee, Yang and Parr (LYP) [35]. Of necessity, the relatively modest split-valence

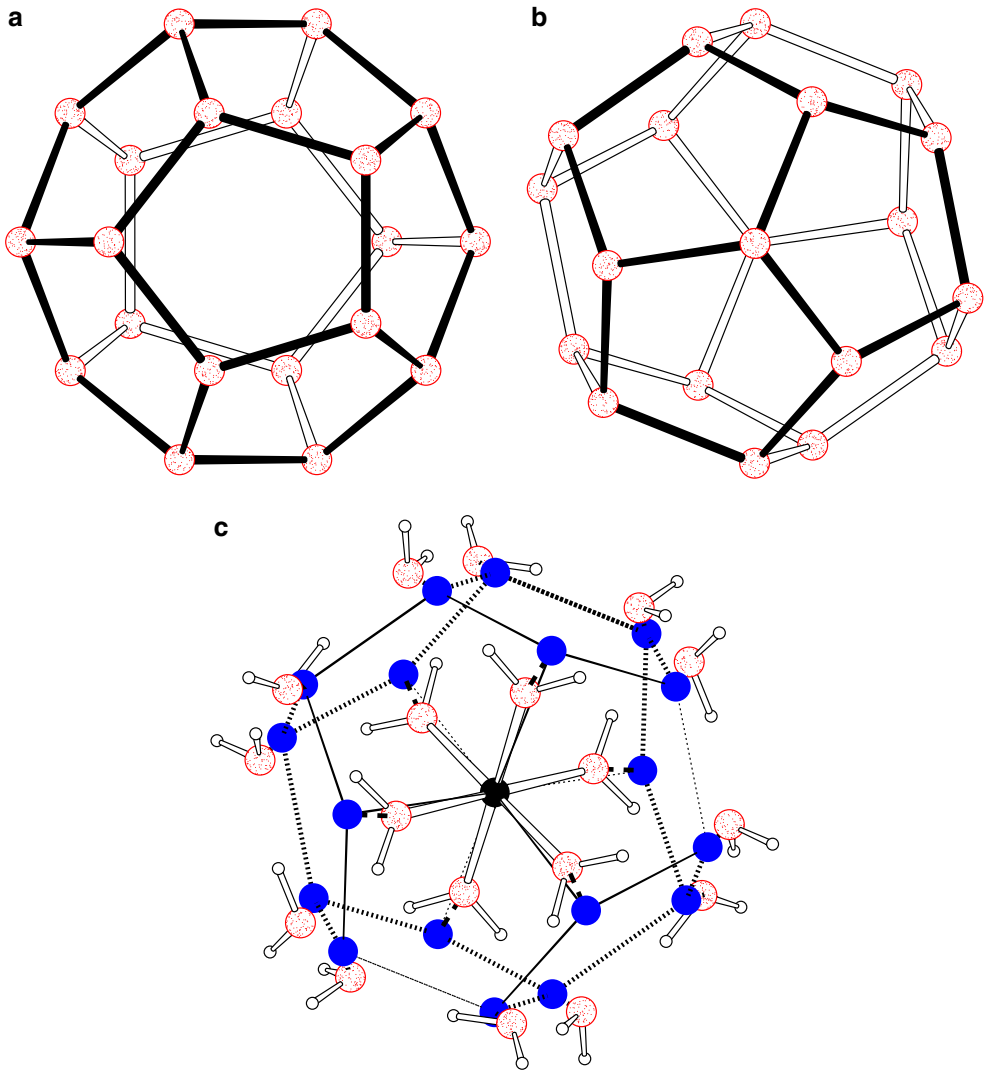


**Fig. 3** The crystal structure of a regular dodecahedral arrangement of water molecules surrounding chlorine (not shown) [50,51]. **(a)** Chlorine hydrate viewed onto one of the dodecahedral faces. **(b)** Chlorine hydrate viewed in the orientation of the $Mg\,[H_2O]_6^{2+} \bullet [H_2O]_{12}$ complex in Fig. 2a. **(c)** A superposition of the structure of chlorine hydrate (Fig. 3b) and the $Mg\,[H_2O]_6^{2+} \bullet [H_2O]_{12}$ complex (Fig. 2a), showing how the 12 second-shell water molecules coincide with many of the 20 apices of the chlorine hydrate dodecahedron, and how the inner 6 water molecules fill most of the remaining apices but have moved in toward the cation by 1.8–1.9 Å (shown by *broken lines*). The two apical positions directly *above* and *below the center of the diagram* are unfilled by water molecules, but could be filled by them, although the interactions on them are weaker

6-31+G** basis set, which includes a diffuse function on the heavy atoms and polarization functions on all atoms, was used in most cases, although in a few instances we also employed the more complete 6-311++G** basis set [36, 37]. The GAUSSIAN 98 and GAUSSIAN 03 series of programs were used for all the calculations in this article [38, 39]; the CALCALL option was consistently employed. In most cases the initial geometry of the complex was that of the $Mg\,[H_2O]_6^{2+} \bullet [H_2O]_{12}$ ($S_6$) cluster reported by Markham et al. [9] optimized at the B3LYP/6-31+G** level. It is important to note that no symmetry constraints were imposed during the optimizations involving the 18-water clusters, except for a few cases that were intended to reproduce the structures of clusters reported by other authors in which the symmetry was explicitly stated. Indeed, in some cases the symmetry of the cluster clearly changed during the optimization, as did the inner-shell CN. The approximate symmetry group of each 18-water cluster that we investigated was determined using the software package Jaguar 4.1 [40]. Atomic charges were calculated from natural population analyses (NPA), and wave functions were analyzed using natural bond orders (NBOs) [41–43]. The ground electronic states of all the metal ion–water clusters that are discussed in this study are closed-shell singlets.

## 3 Structural database analyses

The Cambridge Structural Database (CSD version 5.26, November 2004 version) [33] was searched for all published

crystal structures involving the cations under study. The program CONQUEST that is connected with the CSD was used [33]. The structures were viewed by use of the graphics program ICRVIEW [44] and the metal ion coordination geometry was evaluated for each structure. Analysis of metric details of coordination geometry was done by the use of the in-house program BANG [45]. The data on cation coordination that we obtained are listed in Table 1.

## 4 Results and discussion

We now describe the results of substituting various metal ions for the central $Mg^{2+}$ ion in the (nearly) $S_6$ structure of $Mg\,[H_2O]_6^{2+} \bullet [H_2O]_{12}$, illustrated in Fig. 2. The relationship of this three-dimensional structure (obtained by us by computational methods) to that of a regular dodecahedron has been described recently by Chaplin [46]. It has been found from X-ray diffraction studies that water molecules can enclose many molecules and ions, forming clathrates [47–49]. An excellent example of the three-dimensional structure of such a clathrate is provided by chlorine ($Cl_2$) hydrate [50,51] which is shown in two orientations in Figs. 3a and b. The oxygen atoms of the water molecules in chlorine hydrate lie at the vertices of a regular dodecahedron; the side lengths are 2.75 Å and the vertices are at a distance of 3.7–3.9 Å from the origin (where the chlorine molecule lies). The $S_6$ structure we found for $Mg\,[H_2O]_6^{2+} \bullet [H_2O]_{12}$ is related to this dodecahedral structure. Twelve of the 20 vertices of a dodecahedron represent positions of oxygen atoms of second-shell water molecules and another six of the vertices represent the oxygen atoms of inner-shell water molecules. However, because of the proximity of the inner-shell water molecules to the metal ion, these six vertices are physically displaced toward the center, distorting the dodecahedron [52]. Thus, the 18 oxygen atoms in our $Mg^{2+}$ reference cluster can be identified with 18 of the 20 vertices of a dodecahedron, as shown in Fig. 3c. The remaining two vertices (directly above and below the center of the diagram in Fig. 3c) could accommodate water molecules but, unlike the other 12 water molecules in the second shell, they cannot directly bond hydrogen to any water molecules in the first shell.

**Table 1** Coordination of metal ions for structures in the Cambridge Crystallographic database

| Metal ion | Total no. entries* | CN4 | CN5 | CN6 |
|---|---|---|---|---|
| All entries with only O, N or S in the first-coordination sphere | | | | |
| $Li^+$ | 1403 | 802 | 132 | 122 |
| $Na^+$ | 1019 | 139 | 196 | 443 |
| $Be^{2+}$ | 46 | 44 | 0 | 0 |
| $Mg^{2+}$ | 476 | 78 | 53 | 316 |
| $Zn^{2+}$ | 2758 | 1151 | 760 | 924 |
| $Al^{3+}$ | 367 | 198 | 47 | 148 |
| $Ti^{4+}$ | 495 | 56 | 127 | 270 |
| Entries with at least one water molecule and only O, N or S in the first-coordination sphere | | | | |
| $Li^+$ | 121 | 96 | 28 | 10 |
| $Na^+$ | 315 | 20 | 71 | 206 |
| $Be^{2+}$ | 8 | 3 | 0 | 0 |
| $Mg^{2+}$ | 202 | 0 | 14 | 184 |
| $Zn^{2+}$ | 526 | 56 | 117 | 354 |
| $Al^{3+}$ | 32 | 0 | 3 | 28 |
| $Ti^{4+}$ | 15 | | 2 | 13 |
| Entries with only water molecules in the innermost coordination shell | | | | |
| Li | | 20 | 1 | 1 |
| Na | | 2 | 2 | 15 |
| Be | | 3 | 0 | 0 |
| Mg | | 0 | 0 | 79 |
| Zn | | 0 | 1 | 24 |
| Al | | 0 | 0 | 12 |
| Ti | | 0 | 0 | 0 |

CN Coordination number

* This is the total number of entries ("refcodes" in the CSD. crystal structures reported in the literature) for all coordination numbers that have at least an O and/or N and/or S surrounding the metal ion. If the structure (individual CSD refcode) contains multiple metal ions per asymmetric unit that entry will appear in two or more places in the "CN4 CN5 CN6" columns.

*Aluminum ($Al^{3+}$):* The first substitution that we consider is the replacement of divalent magnesium by trivalent aluminum. In aqueous solution, a hydrated $Al^{3+}$ ion is known to be six-coordinate [53–55]; the long mean resonance time (MRT) of a water molecule in the first shell, approximately 1 s, suggests a metastable structure with a substantial energy barrier to water exchange [22]. Calculations at a variety of computational levels [10] have shown that an $Al\,[H_2O]_6^{3+}$ cluster with $T_h$ symmetry is a local minimum on the PES. However, a four-coordinate structure of the form $Al\,[H_2O]_2\,[OH]_2^+ \bullet \left[H_3O^+\right]_2$ was determined to be 11.8 kcal/mol lower in energy at the B3LYP/6-31+G** level. This finding is in accord with gas-phase experiments that have shown the instability of $Al\,[H_2O]_n^{3+}$ complexes [56–58]. Although relatively little is known experimentally about the second hydration shell of the $Al^{3+}$ ion, estimates from X-ray diffraction and MD simulations give second-shell CNs that range from 12 to 14 [53–55,59].

Rudolph et al. [60] found that an $Al\,[H_2O]_6^{3+} \bullet [H_2O]_{12}$ cluster with $T$ symmetry was a local minimum on the PES at the HF/6-31G* level, and our more recent calculations at the B3LYP/6-31+G** level agree with this finding [10]. We also showed that an $Al\,[H_2O]^{3+} \bullet [H_2O]_{12}$ cluster with $T_h$ symmetry is a sixth-order transition state at this level [10]. When we replaced the $Mg^{2+}$ ion in our $S_6$ structure with an $Al^{3+}$ ion and reoptimized the geometry, a local minimum with $S_6$ symmetry was found which is 3.7 kcal/mol lower in energy than the $T$ structure at the B3LYP/6-31+G** level (see Fig. 2b); the $Al^{3+}$ structure is visually indistinguishable from the $Mg^{2+}$ structure shown in Fig. 2a. Interestingly, the calculated energy difference between the $S_6$ and $T$ forms for the $Al^{3+}$ clusters is less than half the difference for the corresponding $Mg^{2+}$ clusters at the same computational level; this reflects the stronger electrostatic interaction between the surrounding water molecules and $Al^{3+}$, the more highly charged of the two metal ions.

The organization of the hydrogen-bonded network about this hydrated $Al^{3+}$ ion remained essentially the same as in the corresponding $Mg^{2+}$ complex, although, as one would expect based on the smaller ionic radius and higher charge of $Al^{3+}$, the overall structure is more compact; the average Al • • • O distances to a water molecule in the first and second shells are 1.92 and 3.96 Å, respectively (compared with 2.10 and 4.13 Å for the corresponding $Mg^{2+}$ cluster), see Table 2. To obtain a quantitative comparison of the energetic difference between the 18-water networks surrounding $Mg^{2+}$ and $Al^{3+}$, we removed the metal-cation from each of the $S_6$ complexes and performed a single point B3LYP/6-31+G** energy calculation; the network around $Al^{3+}$ is 67.1 kcal/mol higher in energy than the corresponding $Mg^{2+}$ network; the corresponding energy difference between the analogous $T$ clusters is slightly lower, 59.0 kcal/mol. These energy differences provide an indication of the influence that the additional charge of $Al^{3+}$ has on the intrinsic stability of the cluster and shows that the magnesium network is more stable. Presumably this is because the Mg • • • O distance of 2.0–2.1 Å leads to an O • • • O distance of ca. 2.8 Å between adjacent water molecules in the innermost shell (an octahedron), approximately the value found for non-bonded O • • • O interactions in crystal structures [25].

*Zinc ($Zn^{2+}$):* Divalent zinc has a flexible coordination sphere that can accommodate a CN of 4, 5 or 6. When bound to enzymes the CN is typically 4, but during the course of catalysis the CN may increase to 5; the protein-binding sites in which $Zn^{2+}$ is six-coordinate tend to have structural roles [61,62]. A recent analysis of 490 crystal structures in the CSD showed a CN of 4 in 58% of the structures, of 5 in 13%, and of 6 in 27% (C.W. Bock et al. unpublished).

**Table 2** Calculated metal–oxygen distances in coordination spheres in 18-water clusters (Å)

| | CN | Shell | Average | Range |
|---|---|---|---|---|
| Aluminum | 6 | 1 | 1.922 | 1.922 – 1.923 |
| | 6 | 2 | 3.988 | 3.978 – 3.997 |
| Beryllium | 6 | 1 | 1.858 | 1.848 – 4.863 |
| | 6 | 2 | 4.103 | 3.977 – 4.505 |
| Magnesium | 6 | 1 | 2.099 | 2.098 – 2.100 |
| | 6 | 2 | 4.130 | 4.113 – 4.145 |
| Sodium | 6 | 1 | 2.415 | 2.330 – 2.568 |
| | 6 | 2 | 4.184 | 4.034 – 4.371 |
| Titanium | 6 | 1 | 1.993 | 1.715 – 2.143 |
| | 6 | 2 | 4.092 | 3.934 – 4.496 |
| Lithium | 6 | 1 | 2.191 | 2.103 – 2.294 |
| | 6 | 2 | 4.075 | 3.942 – 4.199 |
| Zinc | 6 | 1 | 2.120 | 2.116 – 2.126 |
| | 6 | 2 | 4.123 | 4.057 – 4.162 |
| Beryllium | 4 | 1 | 1.638 | 1.620 – 1.653 |
| | 4 | 2 | 3.672 | 3.525 – 3.765 |
| | 4 | 3 | 4.826 | 4.649 – 4.996 |
| Lithium | 4 | 1 | 1.956 | 1.929 – 2.008 |
| | 4 | 2 | 3.955 | 3.776 – 4.101 |
| | 4 | 3 | 4.808 | 4.648 – 4.961 |
| Sodium | 4 | 1 | 2.279 | 2.252 – 2.341 |
| | 4 | 2 | 4.086 | 3.825 – 4.363 |
| | 4 | 3 | 4.904 | 4.805 – 5.077 |

In aqueous solution $Zn^{2+}$ has a well-defined first hydration shell formed by six-water molecules [63–66]; the MRT of $10^{-7}$ s, for a water molecule in this shell is rather short, consistent with the relative ease of change in CN [22]. Gas-phase clusters of the form $Zn\,[H_2O]_6^{2+}$, $Zn\,[H_2O]_5^{2+} \bullet [H_2O]$ and $Zn\,[H_2O]_4^{2+} \bullet [H_2O]_2$ appear to be relatively close in energy [62,67,68]. We find that a $Zn\,[H_2O]_6^{2+}$ complex with $T_h$ symmetry is a local minimum on the B3LYP/6-31+G** and B3LYP/6-311++G** PESs; however, $Zn\,[H_2O]_4^{2+} \bullet [H_2O]_2$ and $Zn\,[H_2O]_5^{2+} \bullet [H_2O]$ clusters are 5.2 and 2.2 kcal/mol, respectively, lower in energy at the B3LYP/6-31+G** level. In contrast, $Mg\,[H_2O]_6^{2+}$ is 3.4 kcal/mol lower in energy than $Mg\,[H_2O]_4^{2+} \bullet [H_2O]_2$ at this computational level. These energetic differences substantiate the distinct CN preferences of $Mg^{2+}$ and $Zn^{2+}$. It is important to note that MP2 calculations find that a $Zn\,[H_2O]_6$ ($T_h$) is lower in energy than either $Zn\,[H_2O]_4^{2+} \bullet [H_2O]_2$ or $Zn\,[H_2O]_5^{2+} \bullet [H_2O]$ [67,68].[1]

Unfortunately, few experimental data are available concerning the second hydration shell of $Zn^{2+}$. A recent MD simulation puts the number at about 13 [69,70]. Rudolph and Pye [71] found that a structure of the form $Zn\,[H_2O]_6^{2+} \bullet [H_2O]^{12}$ with $T$ symmetry was a local minimum on the PES at the HF/6-31G* level of theory. We now report that this $T$-symmetry structure is also a local minimum at the B3LYP/6-31+G** level. Replacing the $Mg^{2+}$ ion with a $Zn^{2+}$ ion in our $S_6$ reference cluster and reoptimizing the geometry yielded a structure that remained six-coordinate and is 8.4 kcal/mol lower in energy than the $T$-symmetry form, see Fig. 4. The symmetry of the cluster decreased during the optimization from nearly $S_6$ for $Mg^{2+}$ to $C_i$ for $Zn^{2+}$, but the pattern of hydrogen bonding remained essentially the same, i.e., all six inner-shell water molecules donate two hydrogen bonds to second-shell water molecules and all twelve second-shell water molecules accept two hydrogen bonds while donating one. The average Zn • • • O distances to the oxygen atoms of the first and second shells, 2.12, and 4.12 Å, respectively, are quite similar to the corresponding Mg • • • O distances. Consistent with the similarity of their water structures, the 18-water cluster without the $Zn^{2+}$ ion is only 1.8 kcal/mol lower in energy than the corresponding cluster without $Mg^{2+}$.

*Beryllium ($Be^{2+}$):* Ab initio studies on beryllium clusters with six water molecules have shown that a structure with all six water molecules in the innermost shell is a local minimum on the PES [72,73]. We also find that such a $Be\,[H_2O]_6^{2+}$ cluster with $T_h$ symmetry is a local minimum on both the B3LYP/6-31+G** and B3LYP/6-311++G** PESs. However, a $Be\,[H_2O]_4^{2+} \bullet [H_2O]_2$ cluster is generally found to be substantially lower in energy [72–74] (C.W. Block, unpublished); at the B3LYP/6-31+G** level this four-coordinate cluster is 32.1 kcal/mol lower in energy than the six-coordinated cluster. Marx et al. [75], using ab initio MD simulations with

[1] Dr. K. S. Kim kindly pointed out to us that the difference between the B3LYP and MP2 results is partly due to the inaccurate treatment of DFT for the exchange repulsions and dispersions needed to accurately describe molecular strains and interactions in clusters.

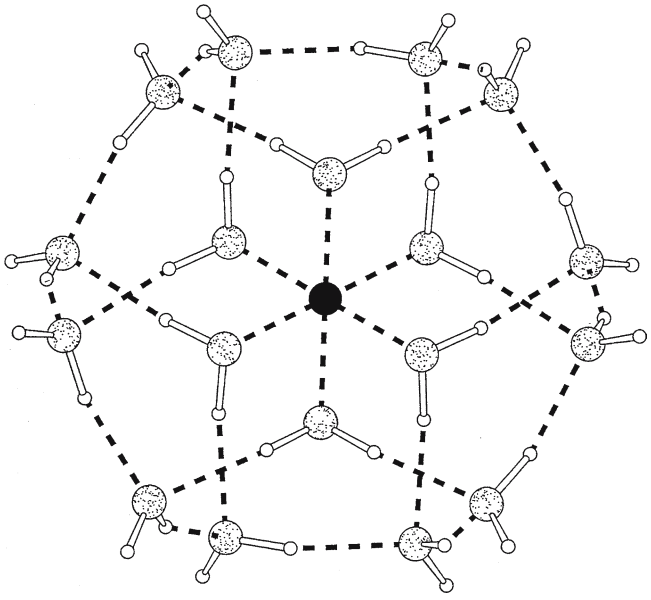

**Fig. 4** Optimized structure of $Zn\,[H_2O]_6^{2+} \bullet [H_2O]_{12}$ obtained at the B3LYP/6-31+G** computational level

gradient-corrected DFT, obtained an analogous result in a 1 ps simulation of a larger ensemble consisting of a $Be^{2+}$ ion and 32 water molecules. They started initially with a configuration in which the divalent beryllium ion was surrounded octahedrally by six water molecules in the first hydration shell. During the simulation two of the water molecules quickly departed from the first hydration shell, resulting in a kinetically stable arrangement with four water molecules in this shell.

X-ray diffraction measurements indicate that $Be^{2+}$ in solution has a CN of four [76]. The MRT of water in the first coordination sphere is rather long for a divalent ion, about $10^{-3}$ s [22]. Structures deposited in the CSD have a CN of four in 44 of the 46 structures containing $Be^{2+}$ with only O, N, and/or S ligands (the other 2 structures have a CN of 3), see Table 1. Little is known experimentally about the number of water molecules in the second shell for $Be^{2+}$, but MD simulations usually predict 8 or 9 [59,77].

When we replaced the $Mg^{2+}$ ion in our $Mg\,[H_2O]_6^{2+} \bullet [H_2O]_{12}$ ($S_6$) cluster (which was optimized at the B3YLP/6-31+G** level) with a $Be^{2+}$ ion and reoptimized the geometry using the B3LYP functional, but with the more complete 6-311++G** basis set, a stable six-coordinated structure was obtained, see Fig. 5a. The average inner-shell Be–O distance, 1.86 Å, is quite long compared to the average Be • • • O distance obtained from the four coordinate crystal structures in the CSD, 1.64 Å . Such long Be • • • O distances in this six-coordinated structure are necessary to reduce repulsions between water molecules surrounding the very small $Be^{2+}$ ion (ionic radius only 0.31 Å), but these occur at the expense of diminished metal ion–oxygen interactions.

There are significant differences in the hydrogen-bonded network of the $Be\,[H_2O]_6^{2+} \bullet [H_2O]_{12}$ cluster in comparison to the clusters in which the metal ion is $Mg^{2+}$, $Zn^{2+}$ or $Al^{3+}$.

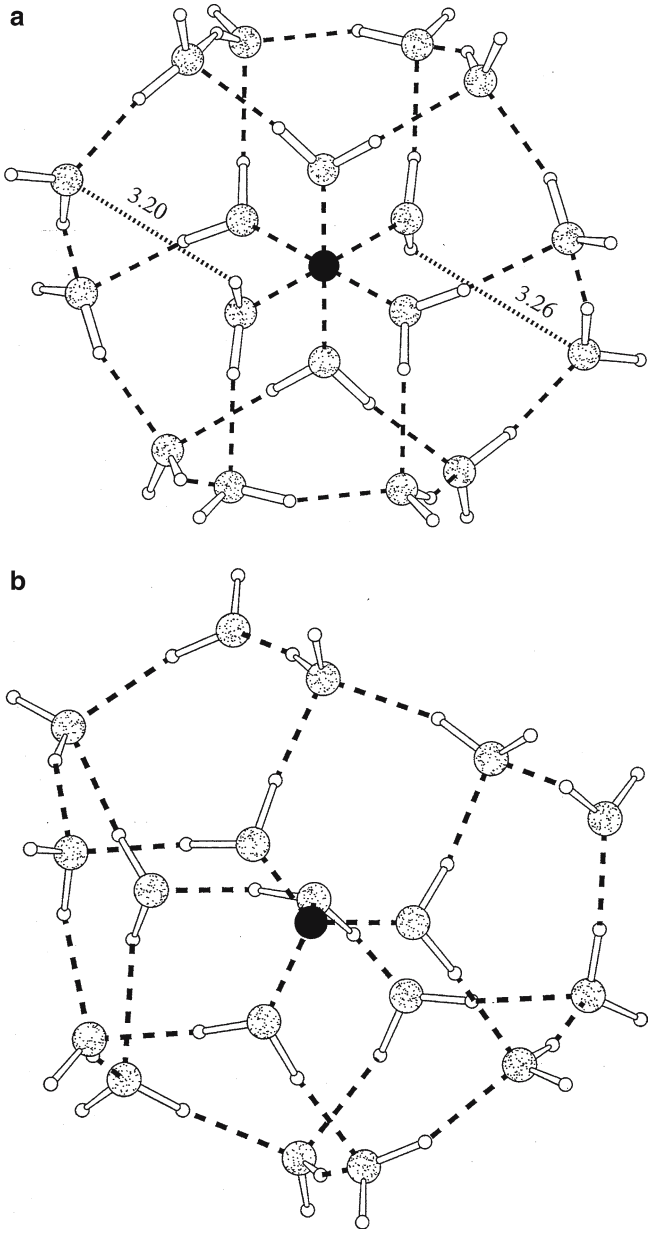


**Fig. 5** Optimized structure of **(a)** $Be\,[H_2O]_6^{2+} \bullet [H_2O]_{12}$ and **(b)** $Be\,[H_2O]_4^{2+} \bullet [H_2O]_8 \bullet [H_2O]_6$ obtained at the B3LYP/6-311++G** and B3LYP/6-31+G** computational levels, respectively

Specifically, the symmetry of this $Be^{2+}$ cluster changed from $S_6$ to $C_1$ during the optimization and this is accompanied by changes in the number and nature of the hydrogen bonds among some of the water molecules in the cluster. For example, in the $S_6$ clusters of $Mg^{2+}$, $Zn^{2+}$, and $Al^{3+}$ described above, all 6 inner-shell water molecules donate 2 hydrogen bonds to second-shell water; all 12 second-shell water molecules accept 2 hydrogen bonds (one each from a first- and second-shell water molecules) and donate one (to a second-shell water molecule). One hydrogen atom from each of the second-shell waters is "free" and presumably would form a hydrogen bond to water molecules in the third shell of a more

complete model. In contrast, the $Be\,[H_2O]_6^{2+} \bullet [H_2O]_{12}$ ($C_1$) cluster contains two inner-shell water molecules that donate only one hydrogen bond to a second-shell water molecule. Furthermore, two water molecules in the second shell are involved in only one hydrogen bond as an acceptor and one as a donor; these two waters are about 0.5 Å further from the central $Be^{2+}$ ion than the other ten water molecules. It has been noted that the presence of double hydrogen-bonded structures in pure water clusters is associated with decreased cluster stability [52]. It is also interesting that the average Be•••O distance to the second-shell water molecules in this six-coordinate cluster, 4.10 Å, is only slightly less than the corresponding Mg•••O distance, 4.13 Å, despite the fact that the ionic radius of the $Mg^{2+}$ ion is more than twice as great as the ionic radius of $Be^{2+}$.

Using this $C_1$ form of the cluster as the initial geometry, a further optimization was performed using the B3LYP/6-31+G** level. Interestingly, two water molecules were expelled from the inner shell during the optimization process resulting in a cluster of the form $Be\,[H_2O]_4^{2+} \bullet [H_2O]_8 \bullet [H_2O]_6$ in which there are four water molecules in the first coordination shell and eight water molecules in the second, see Fig. 5b. The symmetry of this form of the cluster is also $C_1$, but its third shell is incomplete in this model. All four first-shell water molecules donate two hydrogen bonds to second-shell water molecules, and the average Be•••O distance in this shell, 1.64 Å, is in reasonable agreement with values from the CSD. The average Be•••O distance to water molecules in the second and third shells are 3.67 and 4.83 Å, respectively, see Table 2.

For comparison we also optimized a cluster of the form $Be\,[H_2O]_4^{2+} \bullet [H_2O]_8$ with no water molecules in the third shell. The average Be•••O distance for first-shell water molecules is 1.63 Å, similar to what we found in the structure described above that has six additional water molecules in the third shell; this clearly illustrates the dominance of electrostatic effects on the geometry of the first shell. The average Be•••O distance to second-shell water molecules is 3.86 Å, somewhat longer than that found in the $Be\,[H_2O]_4^{2+} \bullet [H_2O]_8 \bullet [H_2O]_6$ cluster.

*Lithium ($Li^+$):* X-ray and neutron-scattering data suggest both tetrahedral and octahedral coordinations of a $Li^+$ ion in aqueous solution [78–81]; the MRT of a water molecule in the first coordination shell of $Li^+$, approximately $10^{-8}$ s, reflects a small barrier to any CN change that may occur during the water exchange process. Interpretations of Raman data suggest a hydration number of four [82]; $^1H$ and $^7Li$ NMR studies of aqueous LiCl solutions indicate that the CN changes from 4 to 6 in the temperature range of 30–40 °C [83]. A recent classical MD simulation of aqueous LiCl solution by Egerov et al. [4] showed that the CN of $Li^+$ in such simulations is strongly dependent on the lithium–water potentials employed; their Car–Parrinello simulation which was intentionally started with six water molecules octahedrally distributed around the $Li^+$ ion, degenerated to a four-coordinate structure after only 1 ps. For comparison, we note that there are currently 1,403 $Li^+$ entries in the CSD and nearly 57% of these crystal structures have a CN of 4; approximately 9.4 and 8.7% have the higher CNs of 5 and 6, respectively, see Table 1.

Theoretical studies of small $Li^+$ complexes have generally found that this monovalent ion prefers four water molecules in the inner shell [84, 85], in accord with the crystallographic data in Table 1. We find that a $Li\,[H_2O]_6^+$ cluster with $T_h$ symmetry is a sixth-order transition state at both the B3LYP/6-31+G** and B3LYP/6-311++G** levels. However, a six-coordinate structure with $C_i$ symmetry is a local minimum on the PES.

When the $Mg^{2+}$ ion in our $S_6$ reference structure of $Mg\,[H_2O]_6^{2+} \bullet [H_2O]_{12}$ was replaced with a $Li^+$ ion, and the cluster geometry was reoptimized, the resulting complex remained six-coordinate, although the symmetry changed from $S_6$ to $C_i$, see Fig. 6a, vibrational frequency analysis confirmed that this is a local minimum on the B3LYP/6-31+G** PES. The average Li•••O distances to first- and second-shell water molecules are 2.19 and 4.08 Å, respectively. Interestingly, the inner-shell Li•••O distance in this cluster is about 0.09 Å longer than the Mg•••O distance for the $Mg^{2+}$ reference cluster, whereas the second shell Li•••O distance is about 0.05 Å shorter than the analogous Mg•••O distance. Thus, the hydrogen bonding among water molecules in the $Li^+$ complex is tighter than it is in the $Mg^{2+}$ complex; the 18-water network surrounding hexacoordinate $Li^+$ is 20.8 kcal/mol higher in energy than the corresponding network surrounding $Mg^{2+}$, despite the comparatively long Li•••O distances in the first shell.

The structure of the hydrogen bonding network in $Li\,[H_2O]_6^+ \bullet [H_2O]_{12}$ differs from those of the analogous $Mg^{2+}$, $Zn^{2+}$, and $Al^{3+}$ clusters in that two of the inner-shell water molecules donate only one hydrogen bond to a second-shell water, but they also accept one hydrogen bond from a second-shell water; the Li•••O distances for these two water molecules, 2.29 Å, are longer than for the other four water molecules in the inner shell. Furthermore, two of the water molecules in the second shell have no free hydrogen atoms with which to form hydrogen bonds to water molecules in the third shell.

Since experimental data for $Li^+$ solutions suggest that it may adopt an inner-shell CN of four in aqueous media, we performed an additional optimization initiated from the structure of the $Be\,[H_2O]_4^{2+} \bullet [H_2O]_8 \bullet [H_2O]_6$ model described above, but with the $Be^{2+}$ ion replaced by a $Li^+$ ion. The first-shell CN of the resulting $Li^+$ cluster remained at four, see Fig. 6b, and the average Li•••O distance to a water molecules in this shell is 1.96 Å, about 0.2 Å shorter than that found in the analogous six-coordinated cluster, reflecting less steric hindrance to the approach. There are also some significant differences in the structure of the hydrogen-bonded network in this four-coordinate cluster compared to that of $Be\,[H_2O]_4^{2+} \bullet [H_2O]_8 \bullet [H_2O]_6$, e.g., one of the four water molecules in the inner shell not only donates two hydrogen bonds to water molecules in the second shell, but also accepts one hydrogen bond. Furthermore, the number of water molecules in the second shell increased from 8 to 9

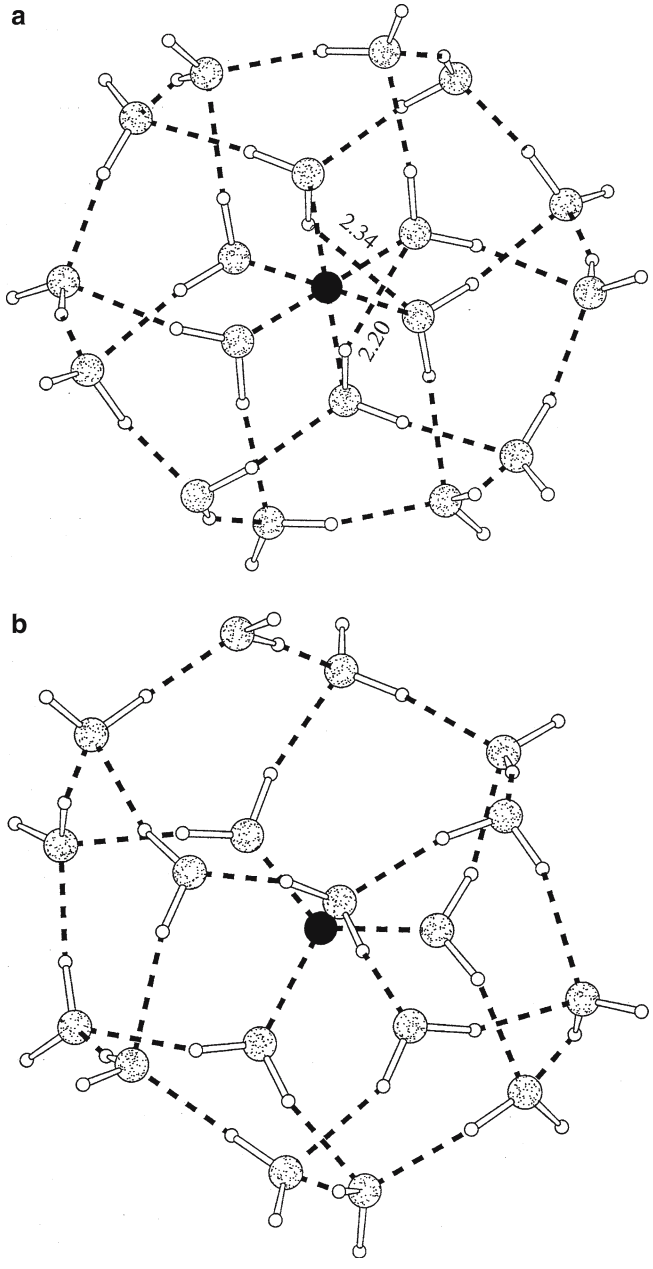


**Fig. 6** Optimized structures of **(a)** $Li\,[H_2O]_6^+ \bullet [H_2O]_{12}$ and **(b)** $Li\,[H_2O]_4^+ \bullet [H_2O]_9 \bullet [H_2O]_5$ obtained at the B3LYP/6-31+G** computational level

during the optimization. This $Li\,[H_2O]_4^+ \bullet [H_2O]_9 \bullet [H_2O]_5$ complex is lower in energy than the six-coordinate complex, but the difference is rather small, 2.1 kcal/mol. As would be expected, the conversion from $Li\,[H_2O]_6^+ \bullet [H_2O]_{12}$ to $Li\,[H_2O]_4^+ \bullet [H_2O]_9 \bullet [H_2O]_5$ is entropically favored, but $\Delta S$ is only 5.2 cal/mol-K.

*Sodium ($Na^+$):* A sodium cation, surrounded by a total of six water molecules, has been extensively studied by computational methods [86–89]. We find that a cluster of the form $Na\,[H_2O]_6^+$ with $T_h$ symmetry is a third-order transition state on the B3LYP/6-31+G** and B3LYP/6-311++G** PESs, whereas a structure with $S_6$ symmetry is a local minimum. However, Kim et al. [86] found that a $Na\,[H_2O]_4^+ \bullet [H_2O]_2$ cluster is the global minimum on the PES using MP2 methodology with double and triple zeta quality basis sets at low temperatures, whereas $Na\,[H_2O]_5^+ \bullet [H_2O]$ is most stable near room temperature [86]. At the B3LYP/6-31+G** level, we also find that $Na\,[H_2O]_4^+ \bullet [H_2O]_2$ is the lowest-energy form; $Na\,[H_2O]_5^+ \bullet [H_2O]$ and $Na\,[H_2O]_6^+$ ($S_6$) are 4.1 and 5.9 kcal/mol, respectively, higher in energy.

In a recent QM/MM molecular dynamics simulation of a $Na^+$ ion in 199 water molecules, Tongraar and Rode [8] found an average inner-shell CN of 5.4. They also found that, compared to pure $H_2O$, water molecules in the first hydration shell of $Na^+$ are quite strongly attached to the ion implying that $Na^+$ acts as a "structure-making" ion; nevertheless the MRT of a water molecule in the first coordination sphere is only ca. $10^{-9}$ s. In contrast, water molecules in the first hydration shell surrounding the larger $K^+$ ion were found to be very labile, consistent with $K^+$ acting more as a "structure-breaking" ion [8]. In a recent Car–Parrinello MD simulation of a $Na^+$ $Cl^-$ ion pair in 48 water molecules, Khalack and Lyubartsev [90] report a CN for $Na^+$ of 4.9 in the so-called water-mediated state (the CN was 5.6 for the corresponding $Cl^-$ counterion). The CN of $Na^+$ in aqueous media measured by diffraction methods is distributed from 4 to 8 [91–95]. Relatively little is known about the second hydration shell of $Na^+$, although an early MD simulation estimated it as 12.4 [96]. Table 1 reports that of the 1,019 structure-containing $Na^+$ in the CSD, 43% have a CN of 6; the average distance of $Na^+$ to the oxygen atom of the waters in the first and second shells is 2.42 and 4.18 Å, respectively; the preference for a CN of 6 is even more pronounced (15 of 19 entries) when the subset of 160 structures with only water in the first coordination shell is considered (Table 1c).

The optimized structure of the hydrated $Na^+$ ion, obtained by replacing the $Mg^{2+}$ ion in the $S_6$ reference cluster remained six-coordinated, see Fig. 7a, although the symmetry decreased to $C_1$. The average $Na \bullet\bullet\bullet O$ distances to first- and second-shell water molecules are 2.42 and 4.18 Å, respectively, the longest observed in our study; the range of $Na \bullet\bullet\bullet O$ distances, 2.33–2.57 Å and 4.03–4.37 Å, is very broad, suggesting that the $Na \bullet\bullet\bullet O$ interaction is relatively weak. This is consistent with the large ionic radius of $Na^+$. Indeed a nascent hydrogen bond between the two first shell waters can be seen. The energy of the 18-water cluster at the geometry of the $Na^+$ complex is 65.4 kcal/mol lower than the corresponding water structure around the $Mg^{2+}$ complex.

Since experimental data are not definitive with respect to the inner-shell coordination number of $Na^+$, we initiated an optimization of a cluster by exchanging the cation in the $Li\,[H_2O]_4^+ \bullet [H_2O]_9 \bullet [H_2O]_5$ structure described above. The resulting cluster remained four-coordinate with nine water molecules in the second shell, see Fig. 7b. This $Na\,[H_2O]_4^+ \bullet [H_2O]_9 \bullet [H_2O]_5$ cluster is 0.4 kcal/mol higher in energy than the six-coordinate structure. The average $Na \bullet\bullet\bullet O$ distance to first- and second-shell water molecules are 2.28 and 4.09 Å,

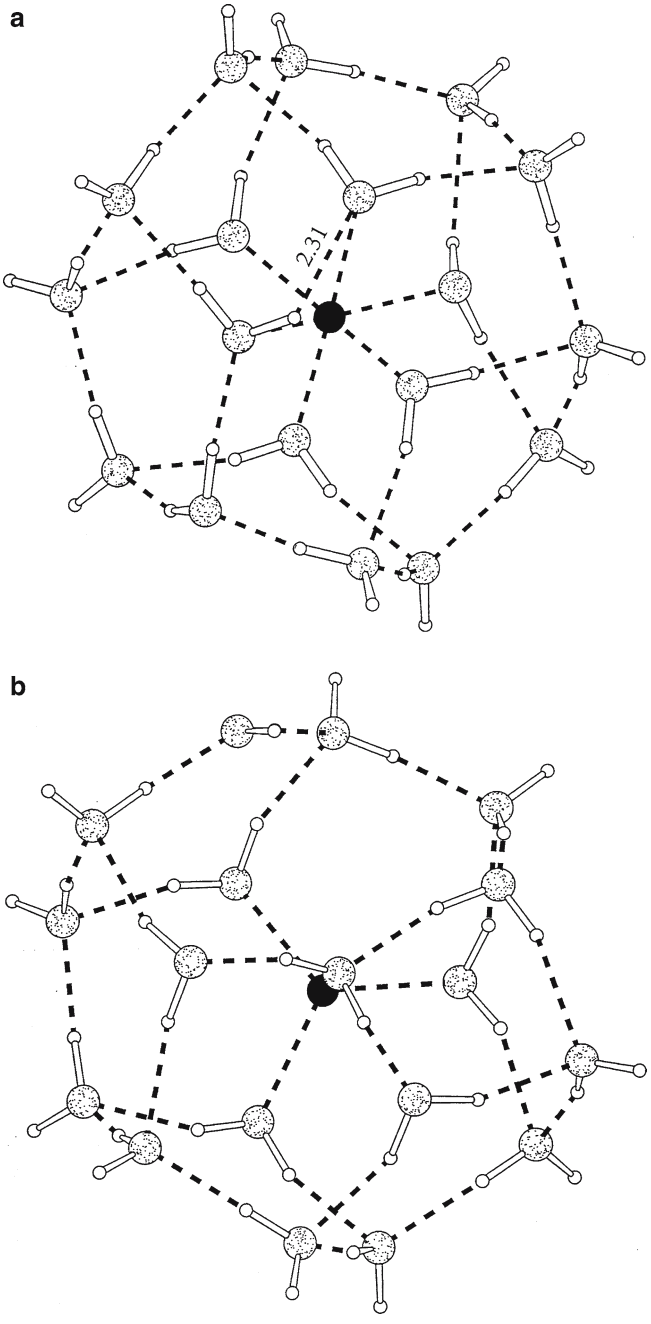


**Fig. 7** Optimized structures of **(a)** $Na\,[H_2O]_6^+ \bullet [H_2O]_{12}$ and **(b)** $Na\,[H_2O]_4^+ \bullet [H_2O]_9 \bullet [H_2O]_5$ obtained at the B3LYP/6-31+G** computational level

respectively; both of these distances are shorter than the corresponding distances in the six-coordinate structure.

*Titanium ($Ti^{4+}$):* Uudsemaa and Tamm [11] showed that a complex of the form $Ti\,[H_2O]_6^{4+}$ with $T_h$ symmetry is a local minimum on the PES; we have also confirmed this at the B3LYP/6-31+G** level. However, in view of the large charge on the $Ti^{4+}$ ion, it is unlikely that this is the global minimum on the PES [10,56–58,97]. These authors were also the first to study the structure of the second hydration shell surrounding this tetravalent cation. In accord with the known behavior of $Ti^{4+}$ ions in solution, chemical hydrolysis was observed and three protons were transferred to the outermost water molecules giving a structure that could be described as a $Ti\,[H_2O]_3\left[OH^-\right]_3^+ \bullet [H_2O]_9 \bullet \left[H_3O^+\right]_3$ cluster. In contrast, such hydrolysis was not observed for the corresponding $Ti^{3+}$ and $Ti^{2+}$ clusters, where $Ti\,[H_2O]_6^{n+} \bullet [H_2O]_{12}$ structure with (nearly) $S_6$ symmetry were found to be lowest in energy.

Starting from our $S_6$ reference structure of $Mg\,[H_2O]_6^{2+} \bullet [H_2O]_{12}$, replacing $Mg^{2+}$ by $Ti^{4+}$ and reoptimizing, also resulted in hydrolysis. The cluster remained six-coordinate, but only a single proton was transferred from an inner-shell water molecule to a second-shell water molecule and an $H_3O^+ \bullet\bullet\bullet H_2O$ moiety was expelled from the complex. We terminated the optimization when the $H_3O^+ \bullet\bullet\bullet H_2O$ unit was approximately 14 Å from the central titanium ion, see Fig. 8 (the $H_3O^+ \bullet\bullet\bullet H_2O$ moiety is not shown in the diagram). The $Ti\bullet\bullet\bullet O$ distance to the hydroxyl group in the first shell, 1.72 Å, is short compared to the average $Ti\bullet\bullet\bullet O$ distance to the five water molecules in the inner shell, 2.05 Å; this hydroxyl group forms a strong hydrogen bond with one water molecule in the second shell; the $H\bullet\bullet\bullet O$ distance is 1.56 Å.

We also performed an optimization initiated from the Uudsemaa and Tamm [11] structure of the complex (T. Tamm, private communication) described in [11]. Again, an $H_3O^+ \bullet\bullet\bullet H_2O$ moiety dissociated from the cluster and the

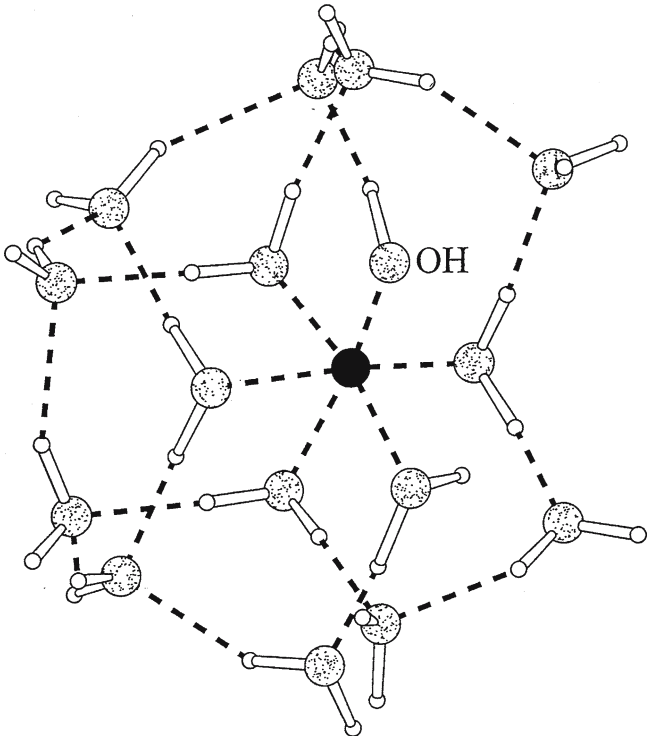


**Fig. 8** The optimized structure of $Ti\,[H_2O]_6^{4+} \bullet [H_2O]_{12}$ after hydrolysis. The $H_3O^+ \bullet\bullet\bullet H_2O$ moiety is not shown in the diagram

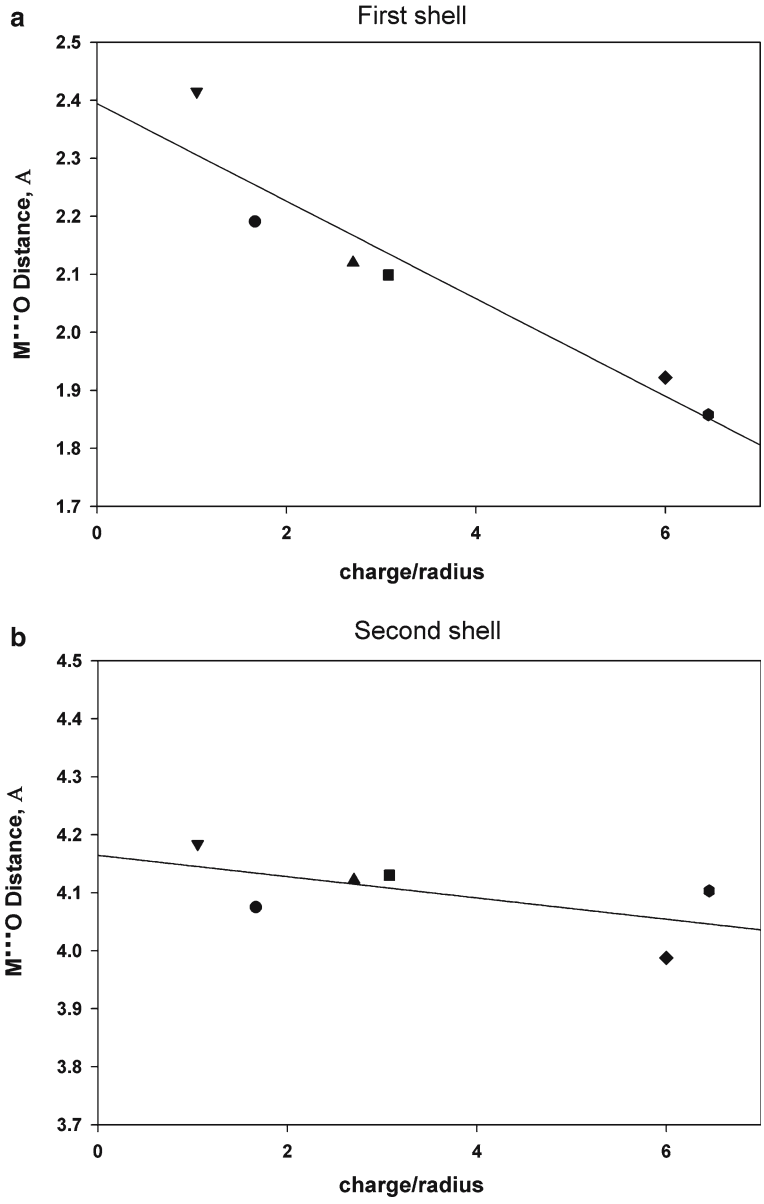


**Fig. 9** Correlation between calculated metal ion–oxygen distances and the charge/radius ratio

optimization was terminated. The origin of the difference between our results and those of Uudsemaa and Tamm [11] is not clear, although different functionals were employed in the two calculations.

## 5 Conclusions

The lowest-energy form that has been found for a cluster composed of 1 $Mg^{2+}$ ion surrounded by 18 water molecules is a $Mg\,[H_2O]_6^{2+} \bullet [H_2O]_{12}$ structure with (nearly) $S_6$ symmetry. It is not yet known if this is the global minimum on the PES. Replacing $Mg^{2+}$ by either $Zn^{2+}$ or $Al^{3+}$ in this $Mg\,[H_2O]_6^{2+} \bullet [H_2O]_{12}$ cluster and reoptimizing the geometry leads to stable complexes that do not radically perturb the pattern of the hydrogen-bonded network present in the $Mg^{2+}$ complex. As would be expected based on electrostatics, the $Mg^{2+}$ and $Zn^{2+}$ clusters are quite similar, whereas the $Al^{3+}$ cluster is more compact. Although no symmetry constraints were actually employed in the optimizations of any of these clusters, nearly symmetrical structures did emerge from the calculations. The symmetry of the clusters appears to decrease from $S_6$ to $C_i$ in going from $Al^{3+} \rightarrow Mg^{2+} \rightarrow Zn^{2+}$ [40].

The effect of ionic radius becomes apparent with the much smaller $Be^{2+}$ ion; the $Be^{2+}$ clusters have a preferred CN of 4 rather than 6, and there is a concomitant restructuring of the hydration shells with the beginning of a third shell.

The structure of the six-coordinate monovalent $M\,[H_2O]_6^{+} \bullet [H_2O]_{12}$ clusters for M = Li and Na is rather different from

those with $Mg^{2+}$, $Zn^{2+}$, or $Al^{3+}$. The cluster with the smaller $Li^+$ ion (radius 0.60 Å) has $C_i$ symmetry, similar to the $Zn^{2+}$ cluster, but the hydrogen-bonding pattern is different in this case. Furthermore, we found a four-coordinate $Li^+$ cluster that is lower in energy. The water molecules surrounding the larger $Na^+$ ion (radius 0.95 Å) are less organized. This is particularly apparent in the range of Na•••O distances for first-shell waters and in the presence of a hydrogen bond between two water molecules in this shell. Furthermore, the analogous four-coordinated $Na^+$ cluster is slightly higher in energy than the six-coordinate complex. In the univalent cation clusters the competing hydrogen-bonding interactions between water molecules play a more important role in determining the dispositions of surrounding water molecules.

At the other extreme, the tetravalent ion $Ti^{4+}$ causes ionization of one of the water molecules in the first coordination shell so that the chemical identity of the complex is altered. This behavior is consistent with experimental data on $Ti^{4+}$ in solution.

The effect of metal charge is apparent when the metal–oxygen distances are referred to the charge/radius ratio of the ion, see Fig. 9. The first-coordination sphere M•••O distances are linearly related to the charge/radius ratio; second-sphere distances are not as well correlated in this way, suggesting an enhanced influence of competing hydrogen-bonding interactions.

In summary, the results of our calculations on the stability of metal water clusters provide insight into the competition between electrostatic, hydrogen bonding, and steric interactions in cation hydration. We have demonstrated the stability of the product of hydration of several ions in the 18-water structures that adopt a regular dodecahedral structure (20 apices) lacking two sites (in this case as far apart as possible). Our results are in accord with the findings of dodecahedral decomposition described by Chaplin [46]. Our extension of these studies to other types of ligands will substantially enhance the understanding of ion selectivity in molecular recognition.

**Acknowledgements** This work was supported by National Institutes of Health grants GM31186, CA10925, CA06927, an appropriation from the Commonwealth of Pennsylvania and a grant NAG8-1826 from NASA. We thank Professor Toomas Tamm, Tallinn University of Technology, EE-19086 Tallinn, Estonia for the coordinates of his $Ti^{4+}$ structures and helpful discussions. The contents of this manuscript are solely the responsibility of the authors and do not necessarily represent the official views of the National Cancer Institute, or any other sponsoring organization.

## References

1. Frausto da Silva JJR, Williams RJP (1991) The biological chemistry of the elements. the inorganic chemistry of life. Clarendon Press, Oxford, England
2. Sigel H, Martin RB (1994) Chem Soc Rev 23:83–91
3. Glusker JP (1991) Adv Protein Chem 42:1–76
4. Egorov AV, Komolkin AV, Chizhik VI, Yushmanov PV, Lyubartsev AP, Laaksonen A (2003) J Phys Chem B107:3234–3242
5. Chillemi G, Barone V, D'Angelo P, Mancini G, Persson I, Sanna N (2005) J Phys Chem B109:9186–9193
6. Schwenk CF, Rode BM (2004) Chem Phys Phys Chem 5:342–348
7. Erras-Hanauer H, Clark T, van Eldik R (2003) Coordination Chem Rev 238–239:233–253
8. Tongraar A, Rode BM (2004) Chem Phys Lett 385:378–383
9. Markham GD, Bock CW, Glusker JP (2002) J Phys Chem B 106:5118–5134
10. Bock CW, Markham GD, Katz AK, Glusker JP (2003) Inorg Chem 42:1538–1548
11. Uudsemaa M, Tamm T (2001) Chem Phys Lett 342:667–672
12. Díaz N, Suárez D, Merz KM Jr (2000) Chem Phys Lett 326:288–292
13. Pavlov M, Siegbahn PEM, Sandstrom M (1998) J Phys Chem A102:219–228
14. Pye CC, Rudolph WW (1998) J Phys Chem A102:9933–9943
15. Caminiti R, Licheri G, Paschina G, Piccaluga G, Pinna G (1980) Z Naturforsch A35:1361–1367
16. Neilson GW, Enderby JE (1983) Proc R Soc Lond A390:353–371
17. Waizumi K, Tamura Y, Masuda H, Oktaki H (1991) Z Naturforsch A46:307–312
18. Pálinkás G, Radnai T, Dietz W, Szrász GI, Heinzinger K (1982) Z Naturforsch A37:1049–1060
19. Jörgensen CK (1957) Acta Chem Scand 11:399–400
20. Matwiyoff NA, Taube H (1968) J Am Chem Soc 90:2796–2800
21. Malinowski ER, Vorgin FJ, Knapp PS, Flint WL, Anton A, Highberger G (1971) J Chem Phys 54:178–181
22. Frey CM, Stuehr J (1974) In: Sigel H (ed) Metal ions in biological systems, vol 1. Marcel Dekker, New York, p 69
23. Johnson CK (1965) Acta Crystallogr 18:1004–1018
24. Pearson RG (1966) Science 151:172–177
25. Bock CW, Kaufman A, Glusker JP (1994) Inorg Chem 33:419–427
26. Vanhouteghem V, Lenstra ATH, Schweiss P (1987) Acta Crystallogr B43:523–528
27. Pavlov M, Siegbahn PEM, Sandstrom M (1998) J Phys Chem 102A:219–228
28. Becke AD (1988) Phys Rev A38:3098–3100
29. Perdew JP (1986) Phys Rev B33:8822–8824
30. Martinez JM, Pappalardo RR, Marcos ES (1999) J Am Chem Soc 121:3175–3184
31. Jorgensen WL, Chandrasekhar J, Madura JD, Impey RW, Klein M L (1993) J Chem Phys 79:926–935
32. Brown ID (1988) Acta Crystallogr B44:545–553
33. Allen FH, Bellard S, Brice MD, Cartwright BA, Doubleday A, Higgs H, Hummelink T, Hummelink-Peters BG, Kennard O, Motherwell WDS, Rodgers JR, Watson DG (1979) Acta Crystallogr B35:2331–2339
34. Becke AD (1993) J Chem Phys 98:1372–1377
35. Lee C, Yang W, Parr RG (1988) Phys Rev B37:785–789
36. Ditchfield R, Hehre WJ, Pople JA (1971) J Chem Phys 54:724–728
37. McLean AD, Chandler GS (1980) J Chem Phys 72:5639–5648
38. Frisch MJ, Trucks GW, Schlegel HB, Scuseria GE, Robb MA, Cheeseman JR, Zakrzewski VG, Montgomery JA, Stratmann RE, Burant JC, Dapprich S, Millam JM, Daniels AD, Kudin KN, Strain MC, Farkas O, Tomasi J, Barone V, Cossi M, Cammi R, Mennucci B, Pomelli C, Adamo C, Clifford S, Ochterski J, Petersson GA, Ayala PY, Cui Q, Morokuma K, Malick DK, Rabuck AD, Raghavachari K, Foresman JB, Cioslowski J, Ortiz JV, Stefanov BB, Liu G, Liashenko A, Piskorz P, Komaromi I, Gomperts R, Martin RL, Fox DJ, Keith T, Al-Laham MA, Peng CY, Nanayakkara A, Gonzalez C, Challacombe M, Gill PMW, Johnson BG, Chen W, Wong MW, Andres JL, Head-Gordon M, Replogle ES, Pople JA (1998) Gaussian 98 (Revision A1), Pittsburgh PA, USA
39. Frisch MJ, Trucks GW, Schlegel HB, Scuseria GE, Robb MA, Cheeseman JR, Montgomery JA Jr, Vreven T, Kudin KN, Burant JC, Millam JM, Iyengar SS, Tomasi J, Barone V, Mennucci B, Cossi M, Scalmani G, Rega N, Petersson GA, Nakatsuji H, Hada M, Ehara M, Toyota K, Fukuda R, Hasegawa J, Ishida M, Nakajima T, Honda Y, Kitao O, Nakai H, Klene M, Li X, Knox JE, Hratchian HP, Cross JB, Bakken V, Adamo C, Jaramillo J, Gomperts R, Stratmann RE, Yazyev O, Austin AJ, Cammi R, Pomelli C, Ochterski

JW, Ayala PY, Morokuma K, Voth GA, Salvador P, Dannenberg JJ, Zakrzewski VG, Dapprich S, Daniels AD, Strain MC, Farkas O, Malick DK, Rabuck AD, Raghavachari K, Foresman JB, Ortiz JV, Cui Q, Baboul AG, Clifford S, Cioslowski J, Stefanov BB, Liu G, Liashenko A, Piskorz P, Komaromi I, Martin RL, Fox DJ, Keith T, Al-Laham MA, Peng CY, Nanayakkara A, Challacombe M, Gill PMW, Johnson B, Chen W, Wong MW, Gonzalez C, Pople JA (2004) Gaussian 03 Revision C02. Gaussian Inc Wallingford CT 2004

40. Jaguar 4.1 (2000) Schrodinger Inc., Portland OR. It should be noted that since no symmetry was actually empoyed in the 18-water cluster optimizations, the symmetry group we are reporting in the text is only approximate and depends on the tolerance used by Jaguar in evaluating the symmetry. For example, our Mg $[H_2O]_6^{2+} \bullet [H_2O]_{12}$ cluster has $S_6$ symmetry for tolerances above about 0.008 Å (the default in Jaguar 4.1 is 0.04 Å), $C_i$ symmetry for tolerances between 0.008 and 0.0006 Å, and $C_1$ below this
41. Reed AE, Curtiss LA, Weinhold F (1988) Chem Rev 88:899–926
42. Reed AE, Weinstock RB, Weinhold F (1985) J Chem Phys 83:735–746
43. Glendening ED, Reed AE, Carpenter JE; Weinhold, F (1995) NBO Version 3.1 from Gaussian 94
44. Erlebacher J, Carrell HL (1992) ICRVIEW – Graphics program for use on Silicon Graphics computers. The Institute for Cancer Research, Fox Chase Cancer Center, Philadelphia, PA, USA
45. Carrell HL (1976) BANG – Molecular geometry program. The Institute for Cancer Research, Fox Chase Cancer Center, Philadelphia, PA, USA
46. Chaplin M, http://www.lbsu.ac.uk/water/equil2.html
47. Powell HM, Riesz P (1948) Nature (London) 161:52–53
48. Jeffrey GA (1969) Acc Chem Res 2:344–352
49. Tsoucaris G (1987) In: Desiraju GR (ed) Organic solid state chemistry Elsevier, Amsterdam, pp 207–270
50. Faraday M (1823) Quant J Sci Let Arts 15:71–74
51. Pauling L, Marsh RE (1952) Proc Natl Acad Sci USA 38:112–118
52. McDonald S, Ojamäe L, Singer SJ (1998) J Phys Chem A102: 2824–2832
53. Bol W, Welzen T (1977) Chem Phys Lett 49:189–192
54. Caminiti R, Licheri G, Piccaluga G, Pinna G, Radnai T (1979) J Chem Phys 71:2473–2476
55. Caminiti R, Radnai T (1980) Z Natruforsch A35:1368–1372
56. Reinhard B, Niedner-Schatteberg G (2002) J Phys Chem A106:7988–7892
57. Siu C-K, Liu Z-F, Tse JS (2002) J Am Chem Soc 124:10846–10860
58. Beyer M, Achatz U, Berg C, Joos S, Niedner-Schatteberg G, Bondybev VE (1999) J Phys Chem A103:671–678
59. Martinez JM, Pappalardo RR, Marcos ES (1999) J Am Chem Soc 121:3175–3184
60. Rudolph WW, Mason R, Pye CC (2000) Phys Chem Chem Phys 2:5030–5040
61. Lipscomb WN, Sträter N (1996) Chem Rev 96:2375–2433
62. Bock CW, Katz AK, Glusker JP (1995) J Amer Chem Soc 117:3754–3763
63. Marcus Y (1998) Chem Rev 88:1475–1498
64. Ohtaki H, Yamaguchi T, Maeda M (1976) Bull Chem Soc Japan 49:701–708
65. Powell DH, Gullidge PMN, Neilson GW (1990) Mol Phys 71:1107–1116
66. Radnai T, Inoue K, Ohtaki H (1990) Bull Chem Soc Jpn 63:3420–3425
67. Mhin BJ, Lee S, Cho SJ, Lee K, Kim KS (1992) Chem Phys Lett 197:77–80
68. Lee S, Kim J, Park JK, Kim KS (1996) J Phys Chem 100:14329–14338
69. Chillemi G, D'Angelo P, Pavel NV, Sanna N, Barone V (2002) J Am Chem Soc 124:1968–1976
70. D'Angelo P, Barone V, Chillemi G, Sanna N, Meyer-Klaucke W, Pavel NV (2002) J Am Chem Soc 124:1958–1967
71. Rudolph WW, Pye CC (1999) Phys Chem Chem Phys 1:4583–4593
72. Bock CW, Glusker JP (1993) Inorg Chem 32:1242–1250
73. Lee MA, Winter NW, Casey WH (1994) J Phys Chem 98:8641–8647
74. Markham GD, Glusker JP, Bock CL, Trachtman M, Bock CW (1996) J Phys Chem 100:3488–3497
75. Marx U, Sprik M, Parrinello M (1997) Chem Phys Lett 273:360–366
76. Yamaguchi T, Ohtaki H, Spohr E, Pálinkás G, Heinzinger K, Probst MM (1986) Z Naturforsch A41:1175–1185
77. Dietz W, Riede W O, Heinzinger K (1982) Z Naturforsch 37A:1038–1048
78. Friedman HL (1985) Chem Scr 25:42–48
79. Ohtaki H, Radnai T (1993) Chem Rev 93:1157–1204
80. Howell I, Neilson GW (1996) J Phys: Condens Matter 8:4455–4463
81. Radnai T, Pálinkás G, Szász GI, Heinzinger K (1981) Z Naturforsch A36:1076–1082
82. Rudolph W, Brooker MH, Pye CC (1995) J Phys Chem 88:3793–3797
83. Chizhik VI (1997) Mol Phys 90:653–660
84. Glendening ED, Feller D (1995) J Phys Chem 99:3060–3067
85. Hashimoto K, Kamimoto T (1998) J Am Chem Soc 120:3560–3570
86. Kim J, Lee S, Cho SJ, Mhin BJ, Kim KS (1995) J Chem Phys 102:839–849
87. Arbman M, Siegbahn H, Pettersson L, Siegbahn P (1985) Mol Phys 54:1149–1160
88. Probst MM (1987) Chem Phys Lett 137:229–233
89. Lybrand TP, Kollman PA (1985) J Chem Phys 83:2923–2933
90. Khalack JM, Lyubartsev AP (2004) Condens Matter Phys 7:683–698
91. Pálinkas G, Radnai T, Hajdu H (1980) Z Naturforsch A35:107–114
92. Ohtomo N, Arakawa K (1980) Bull Chem Soc Jpn 53:1789–1794
93. Maeda M, Ohtaki H (1975) Bull Chem Soc Jpn 48:3755–3756
94. Caminiti R, Licheri G, Paschina G, Piccaluga G, Pinna G (1980) J Chem Phys 72:4522–4528
95. Caminiti R, Licheri G, Piccaluga G, Pinna G (1977) Rend Semin Fac Sci Univ Cagliari XLVI, supp. 19
96. Clementi E, Barsotti R (1978) Chem Phys Lett 59:21–25
97. Puckar L, Tomlins K, Duncombe B, Cox H, Stace AJ (2005) J Am Chem Soc 127:7559–7569